

## Low-Temperature Elasticity and Magneto-Elasticity of Dysprosium Single Crystals

M. ROSEN AND H. KLIMKER

*Nuclear Research Center—Negev, P. O. Box 9001, Beer-Sheva, Israel*

(Received 22 December 1969)

The five independent adiabatic elastic constants of dysprosium have been determined by means of an ultrasonic-pulse technique at a frequency of 10 MHz, between 4.2 and 300°K. The compressional elastic constants  $C_{11}$  and  $C_{33}$  display characteristic anomalies at the magnetic transition points  $T_N$  (178°K) and  $T_C$  (87°K). The shear constants  $C_{44}$  and  $C_{66}$  are very little affected at  $T_N$ ; however, they exhibit typical anomalies at  $T_C$ . The temperature dependence of the directional compressibility  $K_{S11}$  parallel to the hexagonal  $c$  axis is qualitatively a mirror image of the perpendicular compressibility  $K_{SL}$ . Both are only slightly affected at  $T_N$ , but show drastic anomalies at  $T_C$ . At this transition,  $K_{S11}$  exhibits a hardening and  $K_{SL}$  a pronounced softening of the crystal lattice. The limiting Debye temperature extrapolated to 0°K was found to be 190°K. The temperature dependence of the magneto-elastic energy shows a drastic change of 0.71 J  $\text{cm}^{-3}$  at  $T_C$ . Apparently, this change is responsible for the first-order phase transition in dysprosium at  $T_C$ .

### INTRODUCTION

THE low-temperature magnetic properties of polycrystalline dysprosium metal have first been investigated by Trombe.<sup>1</sup> He established a Néel point  $T_N$  of 178°K, and a Curie point  $T_C$  of 85°K. Recent magnetic behavior studies on dysprosium single crystals, by Legvold *et al.*<sup>2,3</sup> have confirmed Trombe's data. Similarly, specific-heat measurements<sup>4</sup> showed the existence of two maxima, at 174 and 84°K. The high-temperature peak displays a definite  $\lambda$  character, and was attributed to the paramagnetic-antiferromagnetic transition, whereas the low-temperature peak indicates the Curie point of dysprosium. Corresponding anomalies were also observed in the electrical<sup>5,6</sup> and thermal<sup>6</sup> conductivities. Magnetization measurements<sup>2</sup> show that dysprosium single crystals are highly anisotropic with spontaneous magnetic moments oriented parallel to the planes of the hexagonal layers. At about 108°K, dysprosium becomes isotropic in the basal plane.<sup>2</sup> At  $T_C$  (85°K) the metal orders spontaneously into a ferromagnetic alignment. It was observed that the  $c$  direction of the hexagonal dysprosium was extremely hard magnetically, the magnetization curves being linear down to the lowest temperatures studied.

Neutron diffraction measurements,<sup>7</sup> in agreement with the magnetization data, have shown a region of spiral antiferromagnetic order from  $T_N$  (178°K) down to  $T_C$  (87°K), with the  $c$  direction of the hexagonal structure as the direction of the spiral axis. Wilkinson *et al.*<sup>7</sup> noted that the magnetization is always in the basal plane but changes in direction from one plane

to the next with a turn angle increasing almost linearly with temperature from 27 to 43° per layer.<sup>8</sup> Below  $T_C$  the magnetic moments are parallel and strongly constrained to the basal plane by a giant crystal field anisotropy<sup>9</sup> of the order of  $10^9$  erg/cm<sup>3</sup>.

Although Banister *et al.*<sup>10</sup> have not found any changes in the crystal symmetry at the Curie point, recent lattice parameter measurements<sup>11,12</sup> indicate sharp discontinuities and distortions in the hexagonal lattice symmetry that can be ascribed to a first-order transition. On the passage from the helical to the ferromagnetic state, at  $T_C$ , the large spontaneous magnetostriction distorts the lattice from hexagonal structure to orthorhombic.<sup>13,14</sup> With decreasing temperature the ratio of the axes changes<sup>11</sup> from  $b/a=1.732=\sqrt{3}$  to 1.720 just below  $T_C$ , to 1.715 at 30°K. Finkel and Vorobev<sup>12</sup> indicated that the occurrence of a maximum, at 145°K, in the temperature dependence of the atomic volume of dysprosium, corresponds to the possibility of a change in the helical structure in this metal.<sup>7,15</sup> The magnetostriction of polycrystalline dysprosium has been measured by Belov *et al.*<sup>16</sup> and by Lee and Alberts<sup>17</sup> who found unusually high values. Even higher values of the magnetostriction constants, with sharp discontinuities at the magnetic ordering temperatures, were observed in single crystals by several workers.<sup>13,14,18</sup>

<sup>8</sup> P. C. Landry, Phys. Rev. **156**, 578 (1967).

<sup>9</sup> J. J. Rhyne and A. E. Clark, J. Appl. Phys. **38**, 1379 (1967).

<sup>10</sup> J. R. Banister, S. Legvold, and F. H. Spedding, Phys. Rev. **94**, 1140 (1954).

<sup>11</sup> F. J. Darnell and E. P. Moore, J. Appl. Phys. **34**, 1337 (1963).

<sup>12</sup> V. A. Finkel and V. V. Vorobev, Zh. Eksperim. i Teor. Fiz. **51**, 786 (1966) [Soviet Phys.—JETP **24**, 524 (1967)].

<sup>13</sup> A. E. Clark, B. F. De Savage, and R. M. Bozorth, Phys. Rev. **138**, A216 (1965).

<sup>14</sup> S. Legvold, J. Alstad, and J. J. Rhyne, Phys. Rev. Letters **10**, 509 (1963).

<sup>15</sup> W. C. Koehler, J. Appl. Phys. **36**, 1078 (1965).

<sup>16</sup> K. P. Belov, R. Z. Levitin, S. A. Nikitin, and A. V. Pedko Zh. Eksperim. i Teor. Fiz. **40**, 1562 (1961) [Soviet Phys.—JETP **13**, 1096 (1961)].

<sup>17</sup> E. W. Lee and J. Alberts, Proc. Phys. Soc. (London) **79**, 977 (1962).

<sup>18</sup> A. E. Clark, R. M. Bozorth, and B. F. De Savage, Phys. Letters **5**, 100 (1963).

<sup>1</sup> F. Trombe, Compt. Rend. **236**, 591 (1953).

<sup>2</sup> D. R. Behrendt, S. Legvold, and F. H. Spedding, Phys. Rev. **109**, 1544 (1968).

<sup>3</sup> T. T. Jew and S. Legvold, U. S. Atomic Energy Commission Report No. ISP-867, 1963 (unpublished).

<sup>4</sup> M. Griffel, R. E. Skochdopole, and F. H. Spedding, J. Chem. Phys. **25**, 75 (1956).

<sup>5</sup> S. Legvold, F. H. Spedding, F. Barson, and J. F. Elliott, Rev. Mod. Phys. **25**, 139 (1953).

<sup>6</sup> R. V. Colvin and S. Arajs, Phys. Rev. **133**, A1076 (1964).

<sup>7</sup> M. K. Wilkinson, W. C. Koehler, E. O. Wollan, and J. W. Cable, J. Appl. Phys. Suppl. **32**, 48 (1961).

In the vicinity of magnetic ordering points, the spin rearrangements contribute to the total energy of the lattice. Since the elastic constants are second derivatives of the thermodynamic potential with respect to strain, a magnetic contribution is invariably expected at the magnetic transitions. The variation of the elastic moduli and ultrasonic attenuation of polycrystalline dysprosium between 4.2 and 300°K was recently reported.<sup>19</sup> The Néel temperature (178°K) was marked by anomalies in the elastic moduli and ultrasonic attenuation, characteristic of a second-order phase change. However, the drastic jumps in the elastic moduli, adiabatic compressibilities and ultrasonic attenuation in the vicinity of the Curie temperature (86°K) indicated the presence of a first-order phase change. The single-crystal elastic constants of dysprosium, from 298 to 923°K, were measured by Fisher and Dever.<sup>20</sup>

The objective of the present work was to determine the five independent single-crystal elastic constants of dysprosium between 4.2 and 300°K. From the temperature dependence of the elastic constants, the variation of the Debye temperature and adiabatic compressibilities can be calculated. Also, the temperature variation of the magneto-elastic contribution to the total energy in the helical and ferromagnetic states can be derived by using the measured elastic constants and the reported magnetostrictive thermal expansion of dysprosium.<sup>13</sup>

### EXPERIMENTAL DETAILS

The high-purity (99.9%) dysprosium single crystals, supplied by Metals Research Ltd., Cambridge, England, had been prepared by zone melting technique. The crystals were in the form of flat disks, 6 mm in diam and about 5 mm thick. The sample faces were flat and parallel better than 2 parts in 10<sup>4</sup>. The thickness of each crystal disk was measured by means of a calibrated indicator stand to within  $\pm 5 \times 10^{-4}$  mm.

Determination of the five independent elastic coefficients in an hexagonal crystal, namely,  $C_{11}$ ,  $C_{12}$ ,  $C_{13}$ ,  $C_{33}$ , and  $C_{44}$ , requires measurement of acoustic-wave velocities of plane longitudinal waves and appropriately polarized transverse waves propagating along three crystal directions. In the present work, three single crystals were used with the following nominal orientations: crystal *A* with disk axis *z* parallel to the hexagonal *c* axis, crystal *B* with disk axis *z* perpendicular to the hexagonal *c* axis, and crystal *C* with disk axis at an angle  $\phi = 45^\circ$  to the hexagonal *c* axis. X-ray back reflection Laue photographs indicated that the actual crystal orientations were within 2° of the nominal ones. This deviation was accepted as satisfactory, and was neglected in the subsequent computations of the elastic

stiffness coefficients from the experimentally determined acoustic-wave velocities.

The room-temperature specimen density was determined by means of a fluid-displacement technique, using monobromobenzene. The average density of the three single crystals of dysprosium was found to be 8.545 g cm<sup>-3</sup>. The temperature variation of the specimen density, as well as of the acoustical path length, was calculated using the average coefficient of thermal expansion,  $(10.0 \times 10^{-6})^\circ\text{K}^{-1}$ , given by Gschneidner.<sup>21</sup>

The sound-wave velocities were measured by means of an ultrasonic-pulse technique at frequency of 10 MHz. Experimental details and method of data analysis were described elsewhere.<sup>22</sup> Difficulties were encountered in preserving the ultrasonic couplant between the quartz transducers and the dysprosium single crystal through the ferromagnetic transition temperature region. Although, the coupling fluids employed for dysprosium single crystals were identical to those used on polycrystalline specimens,<sup>22</sup> nevertheless much greater care with regard to bond thickness and mode of application, had to be exercised in order to obtain a satisfactory couplant for the entire temperature range, between 4.2 and 300°K. In general, single crystals are more difficult to bond acoustically than polycrystalline samples of the same metal. The behavior of the couplant upon thermal cycling depends to a great extent on the crystal orientation.

Conventional cryogenic and temperature-measuring techniques were used. The samples were slowly cooled to liquid-helium temperature and subsequently warmed to room temperature, at a rate of about 0.5°K min<sup>-1</sup>. The temperature of the sample was determined by means of a helium-gas thermometer and a (Au+Co)-versus-Cu thermocouple, to within 0.5°K.

The elastic constants of a crystal are related to the measured sound-wave velocities through the following equation<sup>23,24</sup>:

$$C_{ij} = \rho V^2,$$

where  $\rho$  is the metal density and  $V$  is the appropriate sound velocity. The detailed relations between the experimentally determined velocities and the elastic constants of hexagonal crystals are given in Table I. The velocities  $V_1$ ,  $V_2$ ,  $V_3$ ,  $V_5$ , and  $V_{QL}$  were used for the calculation of the elastic constants  $C_{33}$ ,  $C_{44}$ ,  $C_{11}$ ,  $C_{12}$ , and  $C_{13}$ , respectively. However, the additional sound velocities  $V_4$  and  $V_{QS}$  allowed checking the internal consistency of the experimental data. Thus,  $C_{44}$  of crystal *A* could be compared with  $C_{44}$  of *B*. Similarly,  $C_{13}$  computed from  $V_{QL}$  was compared with  $C_{12}$  from  $V_{QS}$ . The agreement in  $C_{44}$  was better by a factor of 3 than in the  $C_{13}$  elastic coefficients. The total

<sup>21</sup> K. Gschneidner, in *Solid State Physics*, edited by F. Seitz and D. Turnbull (Academic, New York, 1964), Vol. 16, p. 275.

<sup>22</sup> M. Rosen, *Phys. Rev.* **181**, 932 (1969).

<sup>23</sup> M. J. P. Musgrave, *Proc. Roy. Soc. (London)* **A226**, 339 (1954).

<sup>24</sup> J. R. Neighbours, *J. Acoust. Soc. Am.* **26**, 865 (1954).

<sup>19</sup> M. Rosen, *Phys. Rev.* **174**, 504 (1968).

<sup>20</sup> E. S. Fisher and D. Dever, *Trans. AIME* **239**, 48 (1967).

TABLE I. Relation between sound velocities and elastic constants.

	Mode of propagation	Sound velocity equation
Crystal A (disk axis $z$ parallel to hexagonal axis $c$ )	Longitudinal	$\rho V_1^2 = C_{33}$
	Shear	$\rho V_2^2 = C_{44}$
Crystal B (disk axis $z$ perpendicular to hexagonal axis $c$ )	Longitudinal	$\rho V_3^2 = C_{11}$
	Shear	$\rho V_4^2 = C_{44}$
	Shear	$\rho V_5^2 = C_{66} = \frac{1}{2}(C_{11} - C_{12})$
Crystal C [disk axis $z$ at angle $\phi$ ( $45^\circ$ ) to the hexagonal axis $c$ ]	Quasilongitudinal	$2\rho V_{QL}^2 = C_{33} \cos^2\phi + C_{11} \sin^2\phi + C_{44} + \{ [C_{11} \sin^2\phi - C_{33} \cos^2\phi + C_{44}(\cos^2\phi - \sin^2\phi)]^2 + 4 \cos^2\phi \sin^2\phi (C_{13} + C_{44})^2 \}^{1/2}$
	Quasishear	$2\rho V_{QS}^2 = C_{33} \cos^2\phi + C_{11} \sin^2\phi + C_{44} - \{ [C_{11} \sin^2\phi - C_{33} \cos^2\phi + C_{44}(\cos^2\phi - \sin^2\phi)]^2 + 4 \cos^2\phi \sin^2\phi (C_{13} + C_{44})^2 \}^{1/2}$
	Pure shear	$\rho V_{PS}^2 = C_{44} \cos^2\phi + \frac{1}{2}(C_{11} - C_{12}) \sin^2\phi$

estimated error, including internal consistency and geometrical deviations, in the absolute values of the elastic stiffness coefficients  $C_{11}$ ,  $C_{33}$ ,  $C_{44}$ , and  $C_{66}$  is 0.3%. The calculation of  $C_{12}$  from  $C_{66}$  (Table I) leads to an error of 0.6% in  $C_{12}$ . Computation of  $C_{13}$  from  $V_{QL}$  and  $V_{QS}$  is much more elaborate and involves uncertainties in

the elastic constants  $C_{11}$ ,  $C_{33}$ , and  $C_{44}$ , as well as the uncertainty in the angle  $\phi$ . The final accuracy of  $C_{13}$  is estimated to be 2%. The relative, point-to-point, precision of all the elastic stiffness coefficients as a function of temperature is better than the absolute one by a factor of 4.

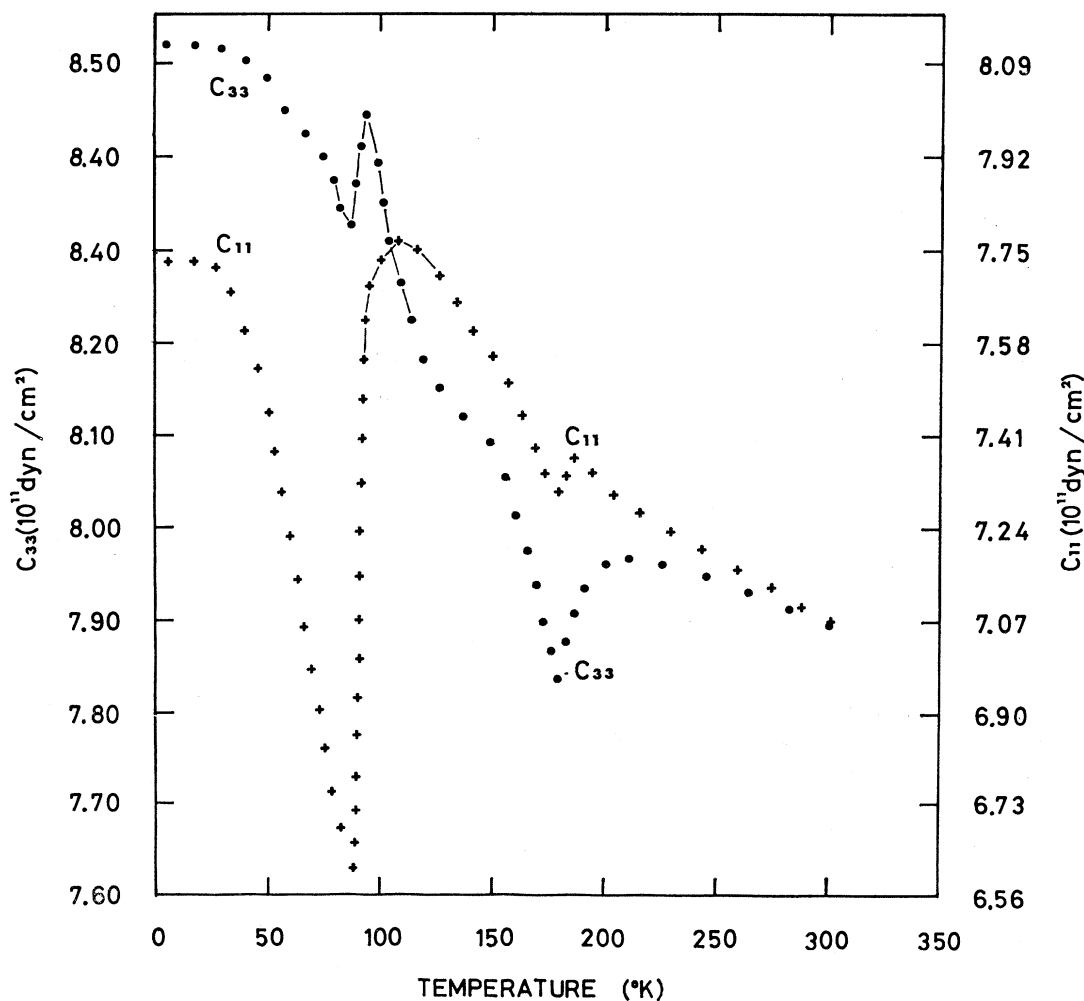


FIG. 1. Temperature dependence of the dilatational elastic coefficients  $C_{11}$  and  $C_{33}$  of dysprosium single crystals.

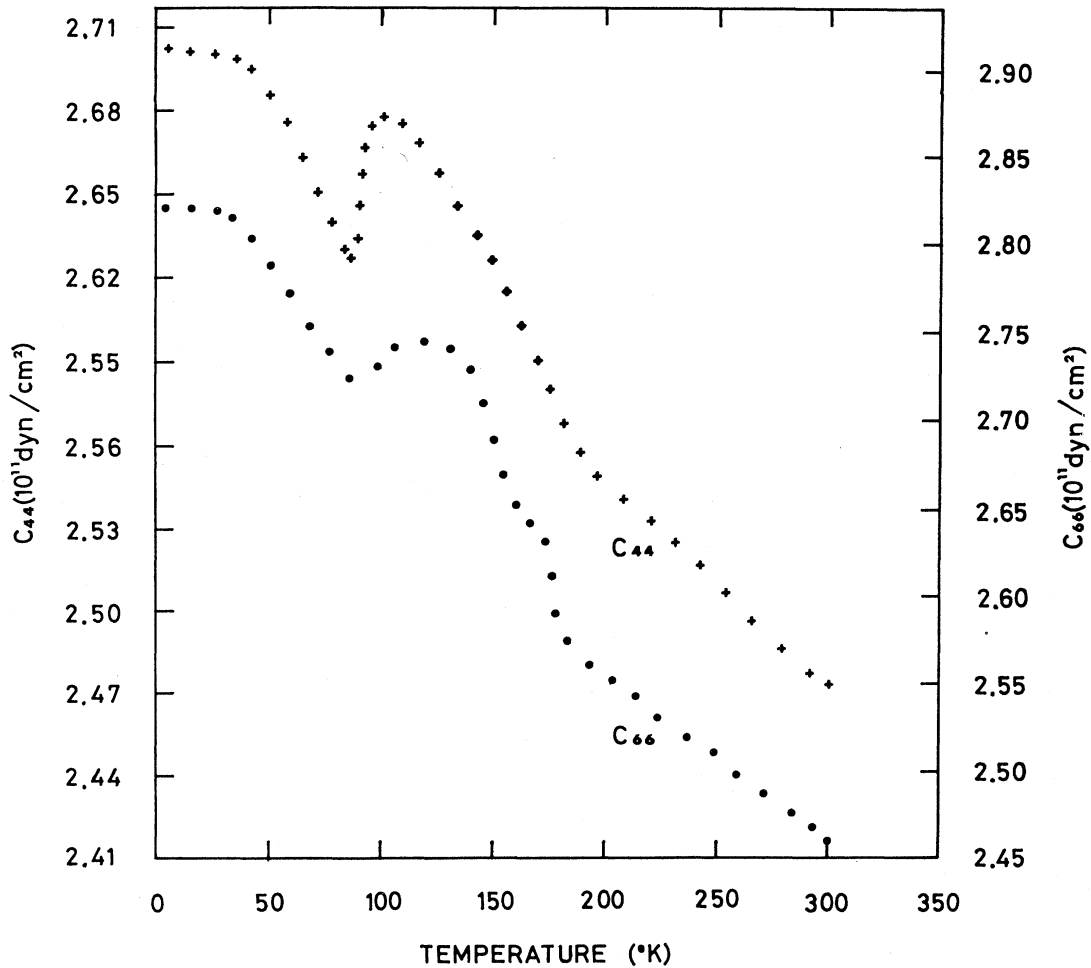


Fig. 2. Temperature dependence of the shear elastic coefficients  $C_{44}$  and  $C_{66}$  of dysprosium single crystals.

RESULTS AND DISCUSSION

The temperature dependence of the dilatational elastic constants of dysprosium is shown in Fig. 1. The compressional sound wave along the hexagonal  $c$  axis yields the  $C_{33}$  elastic constant, while the compressional wave normal to  $c$  gives  $C_{11}$ . Figure 1 illustrates that with decreasing temperature, from the ambient, both  $C_{11}$  and  $C_{33}$  increase in the normal manner, but with different slopes. The elastic constants display typical second-order transition anomalies<sup>25</sup> at the Néel point (178°K). The dip in  $C_{33}$  is more pronounced than in  $C_{11}$ , indicating a relatively larger lattice "softening" along the hexagonal axis during the paramagnetic-helical transition. With further cooling,  $C_{33}$  exhibits a change in slope at about 145°K. At this temperature a maximum in the atomic volume of dysprosium has recently been reported.<sup>12</sup> A possible reason for this behavior may be due to the occurrence of a change in the helical magnetic structure of dyspro-

sium.<sup>7,15</sup> The ferromagnetic transition point, at 87°K, is marked by a drastic softening in  $C_{11}$ ; while  $C_{33}$  is affected to a much smaller extent. It is noteworthy that at  $T_C$  the major anomaly occurs in the  $C_{11}$  elastic coefficient, whereas at  $T_N$  the coefficient  $C_{33}$  is the one which exhibits the larger anomaly.

The temperature dependence of the shear constants  $C_{44}$  and  $C_{66}$  is shown in Fig. 2. Both moduli are very little affected at  $T_N$ , except for change in slope. However, at  $T_C$  both  $C_{44}$  and  $C_{66}$  display typical anomalies. In contrast to the shear constants, the cross-coupling coefficients,  $C_{12}$  and  $C_{13}$ , Fig. 3, exhibit sharp anomalies at the magnetic transition points. Particularly spectacular is the 45% decrease in  $C_{12}$  at  $T_C$ .

The absolute values of the elastic coefficients of dysprosium at 298°K can be compared with those reported by Fisher and Dever.<sup>20</sup> The constant  $C_{11}$  and  $C_{33}$  are in agreement within the experimental error of 0.3%. But the absolute values of  $C_{44}$  and  $C_{66}$  from the present measurements are higher by about 1.3%. A possible reason can be a difference in metal purity, or minor variations in the  $c$ -axis orientation of the crystals.

<sup>25</sup> L. D. Landau and E. M. Lifshitz, *Statistical Physics* (Pergamon, New York, 1958), Chap. 14, p. 430.

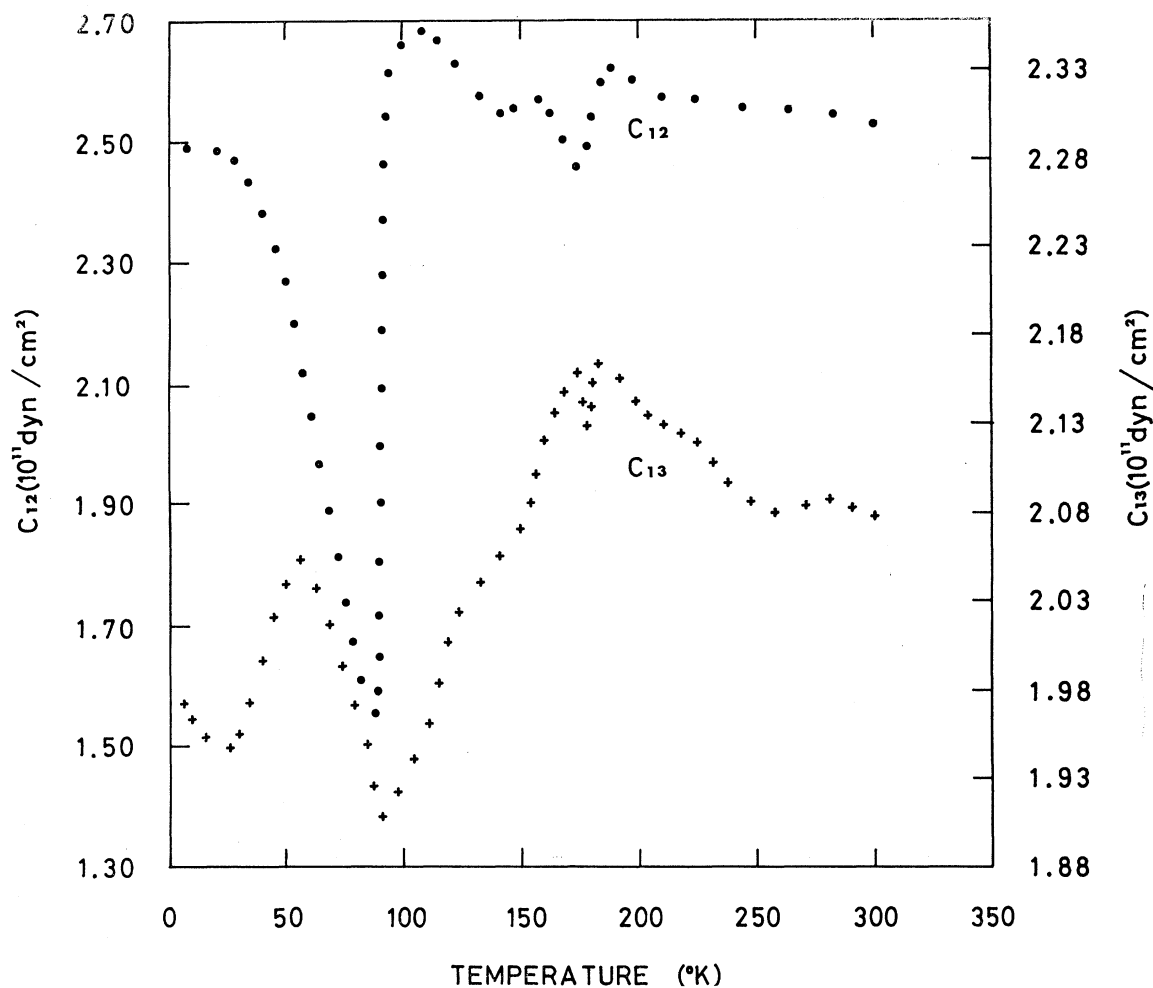


FIG. 3. Temperature dependence of the cross-coupling elastic coefficients  $C_{12}$  and  $C_{13}$  of dysprosium single crystals.

The adiabatic directional compressibilities, parallel ( $K_{S_{11}}$ ) and perpendicular ( $K_{S_{\perp}}$ ) to the hexagonal  $c$  axis, were derived from the computed elastic compliances<sup>26</sup>  $S_{11}$ ,  $S_{12}$ ,  $S_{13}$ ,  $S_{33}$ , and  $S_{44}$ . The directional compressibilities, in term of elastic coefficients are

$$K_{S_{11}} = (C_{11} + C_{12} - 2C_{13}) / [(C_{11} + C_{12})C_{13} - 2C_{13}^2],$$

$$K_{S_{\perp}} = (C_{33} - C_{13}) / [(C_{11} + C_{12})C_{13} - 2C_{13}^2],$$

and the adiabatic volume compressibility

$$K_S(V) = K_{S_{11}} + 2K_{S_{\perp}}.$$

The temperature variation of the directional and volume compressibilities are given in Fig. 4. Qualitatively, the temperature dependence of  $K_{S_{11}}$  is almost the mirror image of  $K_{S_{\perp}}$ . However, the general shape of the volume compressibility curve is dominated by  $K_{S_{\perp}}$ . In the vicinity of room temperature, the absolute values of  $K_{S_{\perp}}$  and  $K_{S_{11}}$  are almost identical. The rate of increase in magnitude of  $K_{S_{\perp}}$  with decreasing tem-

perature is much higher than that of  $K_{S_{11}}$ . In the range between 200°K and room temperature, the change in  $K_{S_{11}}$  is very small. The Néel point of dysprosium, at 178°K, is marked by a small peak in  $K_{S_{\perp}}$ , and a corresponding dip in  $K_{S_{11}}$ . With further decrease in temperature,  $K_{S_{\perp}}$  decreases to its minimum value at about 110°K, and subsequently displays a sharp peak at the Curie temperature of 87°K. This peak corresponds with the pronounced lattice softening at the ferromagnetic transition point of the elastic coefficient  $C_{11}$ , which is the modulus of the compressional wave perpendicular to the hexagonal  $c$  axis. In contrast to  $K_{S_{\perp}}$ ,  $K_{S_{11}}$  exhibits a dip at  $T_C$ , although smaller in magnitude than the peak in  $K_{S_{\perp}}$ . The behavior of the directional compressibilities in dysprosium at  $T_C$ , clearly demonstrates the existence of a lattice "hardening" in the direction parallel to the  $c$  axis, and simultaneously a strong lattice softening in the direction perpendicular to  $c$ .

The ratio of the directional compressibilities  $K_{S_{11}}/K_{S_{\perp}}$ , represents the lattice anisotropy of the crystal.<sup>27</sup>

<sup>26</sup> H. J. McSkimin, J. Appl. Phys. 26, 406 (1955).

<sup>27</sup> J. de Launay, Ref. 21, Vol. 2, p. 219.

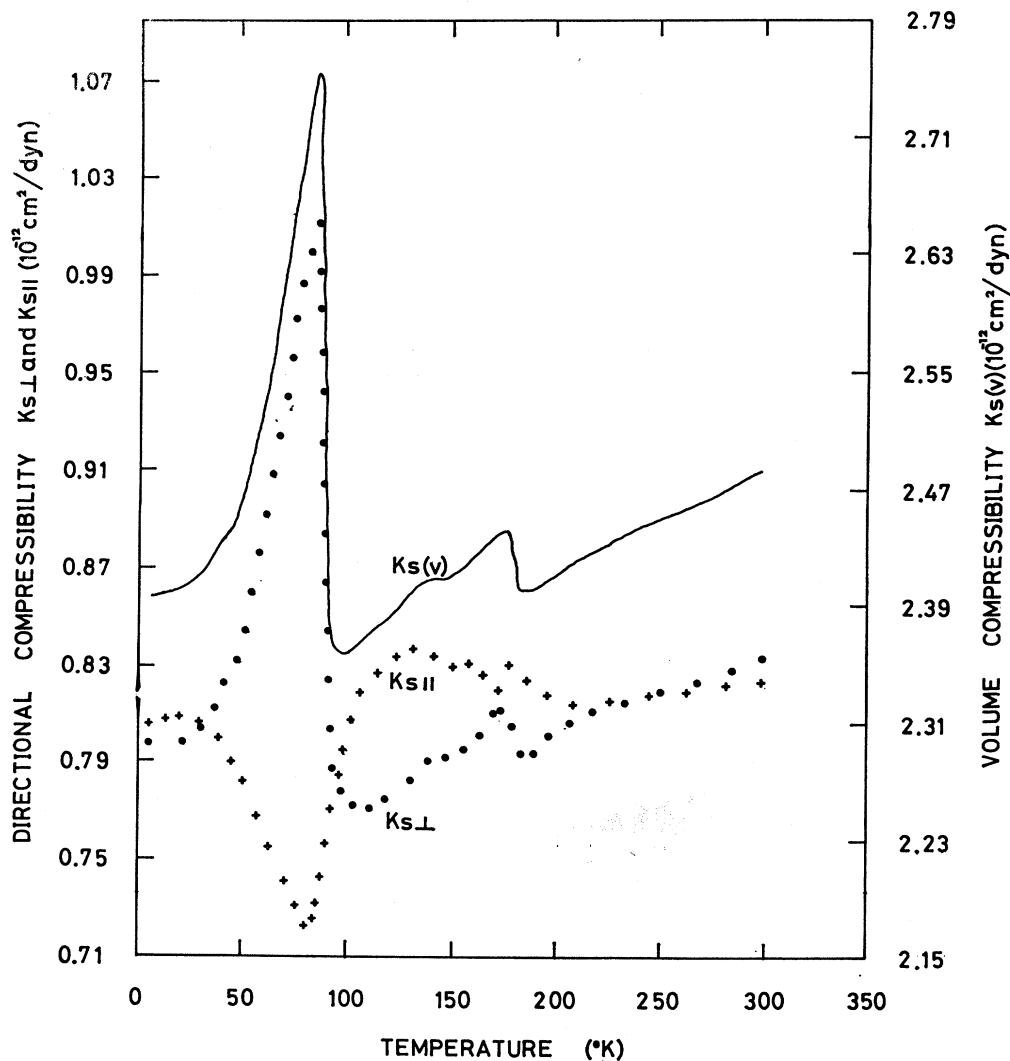


FIG. 4. Temperature dependence of the directional compressibilities  $K_{S\perp}$  and  $K_{S\parallel}$ , and of the volume compressibility  $K_S(V)$  of dysprosium single crystals.

If this ratio is unity, the crystal is elastically isotropic. The temperature dependence of the anisotropy ratio of dysprosium is shown in Fig. 5. In the temperature range from about 200°K to room temperature, the anisotropy ratio is close to unity. The lattice is also fully isotropic in the range between about 35°K and liquid-helium temperature.

The low-temperature elastic constants enable the computation of the Debye temperature,  $\theta_D$ . The elastic  $\theta_D$  is of particular importance for the analysis of thermal properties of magnetically ordered substances that possess a magnetic term in the total heat capacity.  $\theta_D$  is related to the velocity of sound by the equation

$$\theta_D = (\hbar/K_B)(3N\rho/4\pi M)^{1/3}V_m,$$

where  $\hbar$  is Planck's constant,  $K_B$  is Boltzmann's constant,  $N$  is Avogadro's number,  $\rho$  is the metal density,

$M$  is the atomic weight, and  $V_m$  is the mean sound velocity. In the present study, Anderson's velocity-averaging procedure for hexagonal crystals<sup>28</sup> has been employed in order to calculate  $V_m$ , and subsequently,  $\theta_D$ .

The temperature variation of  $\theta_D$  is presented in Fig. 5. Its behavior is similar to that of the elastic coefficients, particularly to the shear constants  $C_{44}$  and  $C_{66}$  (Fig. 2).  $T_C$  is marked by a dip in  $\theta_D$  at 87°K. At more elevated temperatures,  $\theta_D$  varies quite smoothly up to  $T_N$  (178°K), where it changes slope. From  $T_N$  up to room temperature,  $\theta_D$  shows a linear temperature dependence. The value of  $\theta_D$  at room temperature for single-crystal dysprosium (Fig. 5) is 180°K, in agreement with the polycrystalline value<sup>19</sup> of 181°K. The limiting  $\theta_D$ , extrapolated to 0°K, for single crystals is

<sup>28</sup> O. L. Anderson, J. Phys. Chem. Solids 24, 909 (1963).

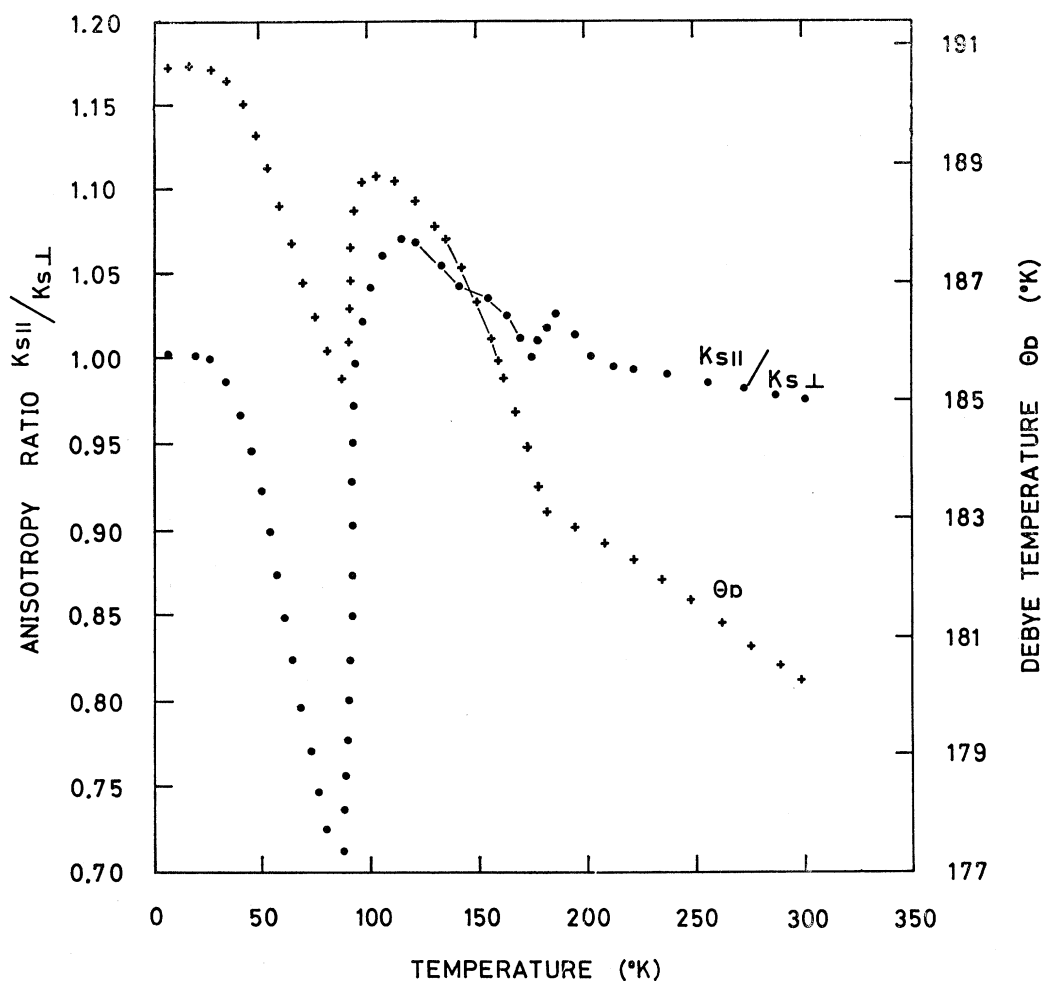


FIG. 5. Temperature dependence of the anisotropy ratio ( $K_{S11}/K_{S1}$ ) and of the Debye temperature ( $\theta_D$ ) of dysprosium single crystals.

190°K, as shown in Fig. 5. This value is higher than the reported 179°K for polycrystalline dysprosium.<sup>19</sup> The discrepancy may be due to the higher metal purity of the single crystals in the present work, as well as to the velocity-averaging procedure. It should be pointed out that both the single-crystal and polycrystalline values of the limiting  $\theta_D$  of dysprosium, i.e., 190 and 179°K, respectively, are higher than the  $\theta_D$  calculated from specific-heat data.<sup>20</sup> The specific heat  $\theta_D$  were reported to be  $(172 \pm 35)$ °K and 158°K, at 0°K and room temperature.

Cooper<sup>30,31</sup> has suggested that the magneto-elastic effect is the driving force for the helical to ferromagnetic transition in dysprosium. In his view, the helical arrangement "clamps" the successive planes along the hexagonal  $c$  axis and prevents development of strains

that would minimize the combined elastic and magnetoelastic energies of the lattice. Thus, the helical state possesses a higher magneto-elastic energy than the ferromagnetic state. At the transition point to the ferromagnetic state, a drastic drop in energy should be expected.

The magnetostriction contribution to the free energy of hexagonal crystals has been treated in detail by Callen and Callen.<sup>32</sup> Evenson and Liu<sup>33</sup> have further developed the theory and have computed the difference in the magneto-elastic energy between the helical and ferromagnetic states at  $T_C$  (85°K). The total magneto-elastic energy, including the elastic and magneto-elastic contributions is as follows:

$$E_{me} = -\frac{1}{2}C_{11}\alpha(\epsilon^{\alpha,1})^2 - \frac{1}{2}C_{22}\alpha(\epsilon^{\alpha,2})^2 - \frac{1}{8}C\gamma(\lambda\gamma)^2,$$

where the last term of the equation is equal to zero in

<sup>19</sup> B. C. Gerstein, M. Griffel, L. D. Jennings, and R. E. Miller, *J. Chem. Phys.* **27**, 384 (1957).

<sup>20</sup> B. R. Cooper, *Phys. Rev. Letters* **19**, 900 (1967).

<sup>31</sup> B. R. Cooper, *Phys. Rev.* **169**, 281 (1968).

<sup>32</sup> E. Callen and H. B. Callen, *Phys. Rev.* **139**, A455 (1965).

<sup>33</sup> W. E. Evenson and S. H. Liu, *Phys. Rev.* **178**, 783 (1969).

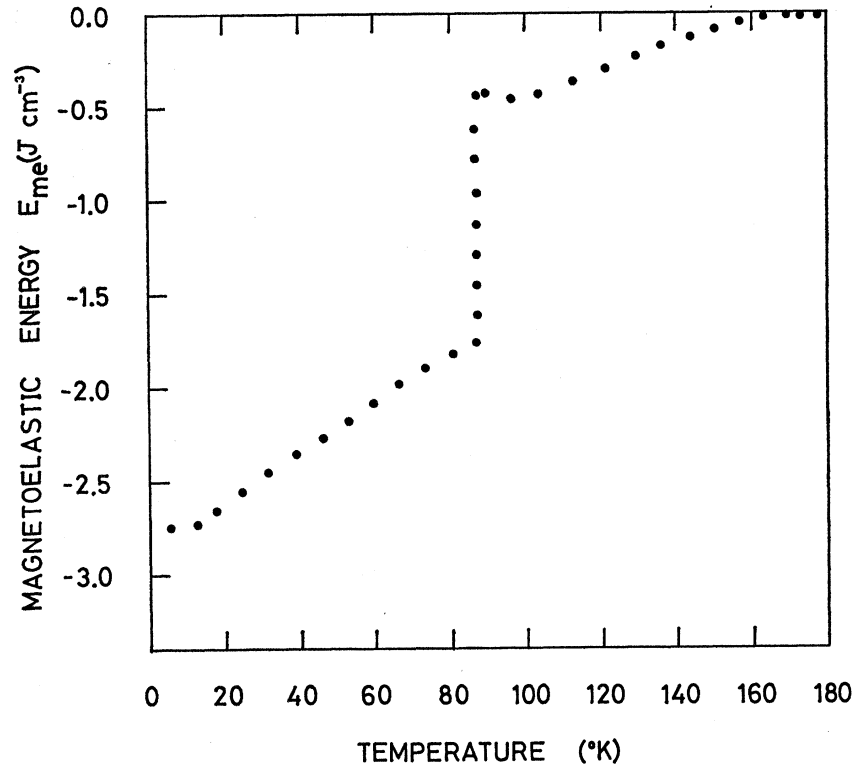


FIG. 6. Temperature dependence of the magneto-elastic energy of dysprosium single crystals in the helical and ferromagnetic states.

the helical state. According to Callen and Callen,<sup>32</sup>

$$\begin{aligned} C_{11}^{\alpha} &= \frac{1}{3}(2C_{11} + 2C_{12} + 4C_{13} + C_{33}), \\ C_{22}^{\alpha} &= \frac{2}{3}(C_{11} + C_{12} - 4C_{13} + 2C_{33}), \\ C^{\gamma} &= 2(C_{11} - C_{12}). \end{aligned}$$

The equilibrium strains are found to be<sup>33</sup>

$$\begin{aligned} \epsilon^{\alpha,1} &= \frac{1}{2}\lambda_1(1 + \cos\psi) - \frac{1}{4}\sqrt{3}(C_{22}^{\alpha}/C_{11}^{\alpha})\lambda_2(1 - \cos\psi), \\ \epsilon^{\alpha,2} &= \frac{1}{4}\lambda_2(1 + 3\cos\psi) - \frac{1}{2}\sqrt{3}(C_{11}^{\alpha}/C_{22}^{\alpha})\lambda_1(1 - \cos\psi), \\ \epsilon_1^{\gamma} &= 0 \text{ in the helical state, and} \\ \epsilon_1^{\gamma} &= \frac{1}{2}\lambda^{\gamma} \text{ in the ferromagnetic state.} \end{aligned}$$

The angle  $\psi$  is the helicomagnetic-turn angle, determined by Landry<sup>8</sup> and found to vary between  $27^{\circ}$  at  $T_C$ , to  $43^{\circ}$  at  $T_N$ . The equilibrium strains  $\epsilon^{\alpha,1}$  and  $\epsilon^{\alpha,2}$  are partially clamped to the helical state. The parameters  $\lambda_1$  and  $\lambda_2$  are defined by Eq. (2.17) of Ref. 33, and are related to the magneto-elastic-coupling coefficients through the elastic constants  $C_{11}^{\alpha}$  and  $C_{22}^{\alpha}$ , respectively. The strains can also be related to the anomalous thermal expansion along the symmetry axes of dysprosium, as measured by Clark *et al.*<sup>13</sup>:

$$\begin{aligned} (\delta l/l)_x &= \frac{1}{3}\epsilon^{\alpha,1} - \frac{1}{3}\sqrt{3}\epsilon^{\alpha,2} + \epsilon_1^{\gamma}, \\ (\delta l/l)_y &= \frac{1}{3}\epsilon^{\alpha,1} - \frac{1}{3}\sqrt{3}\epsilon^{\alpha,2} - \epsilon_1^{\gamma}, \\ (\delta l/l)_z &= \frac{1}{3}\epsilon^{\alpha,1} + \frac{2}{3}\sqrt{3}\epsilon^{\alpha,2}. \end{aligned}$$

Evenson and Liu<sup>33</sup> have calculated the total magneto-elastic energies in the helical and ferromagnetic states

in the vicinity of  $T_C$ . They have used the anomalous thermal expansion data of Clark *et al.*<sup>13</sup> and the single-crystal elastic constants of dysprosium at room temperature.<sup>20</sup> The elastic constants at  $T_C$  were computed by applying the experimental data of the temperature variation of polycrystalline moduli at low temperatures.<sup>19</sup>

Following the theoretical formulation of Evenson and Liu,<sup>33</sup> applying the low-temperature single-crystal elastic stiffness coefficients of dysprosium obtained in the present study, and using the thermal expansions calculated from Darnell and Moore's data,<sup>11</sup> the total magneto-elastic energy was calculated over the entire temperature range of magnetic ordering. The variation of the magneto-elastic energy with temperature is shown in Fig. 6. The energy decreases from zero, at  $T_N$  (178°K), with decreasing temperature. Its value in the helical state just above  $T_C$  (87°K) is  $E_h = -0.42$  J/cm<sup>3</sup>. This value is higher than that estimated by Evenson and Liu,  $-0.72$  J/cm<sup>3</sup>. Just below  $T_C$ , i.e., in the ferromagnetic state, the energy is much smaller,  $E_f = -1.78$  J/cm<sup>3</sup>. The energy drop at  $T_C$  is  $\Delta E = 1.36$  J/cm<sup>3</sup>, compared with  $0.94$  J/cm<sup>3</sup> obtained by Evenson and Liu. Apparently, the drastic change in the magneto-elastic energy at the ferromagnetic transition point is responsible for the first-order phase transformation as exhibited by a change in the crystal symmetry and atomic volume.<sup>11,12</sup>

Figure 6 shows that the magneto-elastic energy decreases with decreasing temperature. The rate of



temperature variation of the magneto-elastic energy is higher in the ferromagnetic state than in the helical state. Noteworthy is the minimum of the magneto-elastic energy in the helical state, at 95°K. At this temperature the volume compressibility, Fig. 4, is at its minimal value.

### ACKNOWLEDGMENTS

The authors are indebted to Professor S. Shtrikman of the Weizmann Institute of Science, Rehovot, Israel for stimulating discussions. The assistance of M. Blau, D. Kalir, A. Halwany, and B. Cohen in the various phases of this work is gratefully acknowledged.

## Coupled Electronic Spins, Nuclear Spins, and Phonons in a Cubic Antiferromagnet\*

PETER A. FEDDERS

*Arthur Holly Compton Laboratory of Physics, Washington University, St. Louis, Missouri 63130*

(Received 26 November 1969)

The spin response functions for the electronic and nuclear spins in a cubic antiferromagnet are obtained in the random-phase approximation. These response functions are then used to investigate the coupled electronic-spin-nuclear-spin-phonon system. Predicted changes in phonon velocity and attenuation in RbMnF<sub>3</sub> due to interaction with electronic and nuclear spin waves are obtained. Some of these predictions agree with previous experiments and theory, and others can be checked by further experiments.

### I. INTRODUCTION

THE coupled system of electronic and nuclear spins<sup>1,2</sup> and its interaction with acoustic phonons<sup>3,4</sup> in an antiferromagnet with cubic symmetry have been of some interest lately. It is the purpose of this paper to treat this coupled problem consistently from a unified point of view within the random-phase approximation (RPA) and, in particular, to obtain detailed predictions for RbMnF<sub>3</sub>. Because of the complicated geometry of the equilibrium magnetization of a cubic antiferromagnet, this treatment is limited to configurations in which an external magnetic field lies in a restricted range of a {110} plane. As will be seen, because of the relatively strong coupling between the electronic and nuclear spins in RbMnF<sub>3</sub>, the combined system must be taken into account in order to obtain correct results for the effects of the antiferromagnetism on the phonons.

The Hamiltonian used to describe the coupled electronic and nuclear spins is

$$H_{en} = \frac{1}{2} \sum_{\alpha, \alpha'} J(\alpha, \alpha') \mathbf{S}(\alpha) \cdot \mathbf{S}(\alpha') - \sum_{\alpha} A \mathbf{I}(\alpha) \cdot \mathbf{S}(\alpha) - \sum_{\alpha} \mathbf{H}_0 \cdot [\mu_e \mathbf{S}(\alpha) + \mu_n \mathbf{I}(\alpha)] + H_a, \quad (1.1)$$

where  $\mathbf{S}(\alpha)$  and  $\mathbf{I}(\alpha)$  are the electronic- and nuclear-spin operators, respectively, at the magnetic site  $\alpha$ . The exchange interaction is written so that  $J(\alpha, \alpha')$  is positive

\* Work supported in part by National Science Foundation under Grant No. GP-9573.

<sup>1</sup> W. J. Ince, Phys. Rev. **184**, 574 (1969).

<sup>2</sup> L. W. Hinderks and P. M. Richards, Phys. Rev. **183**, 575 (1969).

<sup>3</sup> R. L. Melcher and D. I. Bolef, Phys. Rev. **186**, 491 (1969). Hereafter referred to as M & B.

<sup>4</sup> A. Platzker and F. R. Morgenthaler, Phys. Rev. Letters **22**, 1051 (1969).

for antiferromagnetic coupling,  $\mathbf{H}_0$  is a uniform applied magnetic field and  $\mu_e$  ( $\mu_n$ ) is the electronic (nuclear) magnetic moment.  $H_a$  is a term describing the electronic-spin anisotropy energy which, for a cubic system, is

$$E_a = \frac{1}{2} K (S_{x_c}^4 + S_{y_c}^4 + S_{z_c}^4) \quad (1.2)$$

per site. The subscript  $c$  denotes the usual coordinate system coincident with the cubic axes of the crystal.

The spins and phonons interact through the single-ion magnetostriction Hamiltonian  $H_{ep}$  which, for a lattice with cubic symmetry, takes the form

$$H_{ep} = G_{11} \sum_{\alpha} \{ \epsilon_{xx}(\alpha) [S_x^2(\alpha) - \frac{1}{2} S_y^2(\alpha) - \frac{1}{2} S_z^2(\alpha)] + (\text{cyclic permutations}) \} + G_{44} \sum_{\alpha} \{ \epsilon_{xy}(\alpha) \times [S_x(\alpha) S_y(\alpha) + S_y(\alpha) S_x(\alpha)] + (\text{cyclic permutations}) \}. \quad (1.3)$$

The strain components  $\epsilon_{ij}(\alpha)$  can be expressed in terms of the phonon displacement operation  $U_i(\alpha)$  by the equation

$$\epsilon_{ij}(\alpha) = \frac{1}{2} \left[ \frac{\partial U_i(\alpha)}{\partial \alpha_j} + \frac{\partial U_j(\alpha)}{\partial \alpha_i} \right]. \quad (1.4)$$

The method of attacking the problem is to first calculate the electronic-spin correlation function using thermodynamic Green's functions and then to use it to obtain predictions about various experiments. Section II contains a discussion of the model, the approximations employed, and the use of the spin correlation functions. In order (it is hoped) to make the paper more useful to a variety of readers, formulas for the spin correlation functions are derived in Appendix A, while